OXFORD JOURNAL
OF STUDENT
SCHOLARSHIP

Designing & Simulating a TD-UHD Micro-DOT System to Predict Image Resolution Improvement Upon Existing Systems

Cemantha Hearing
cm.hearing@gmail.com

ABSTRACT

Brain activation imaging is an essential component of developing effective treatments for patients affected by neurological conditions. A biomedical imaging system that is currently being used to image brain activation is that of diffuse optical tomography (DOT). DOT, a biophotonic imaging system, has the unique ability to preserve naturalistic environments due to its lightweight structure, but fails at producing high-quality images.

To supplement this issue, ultra-high density (UHD) DOT and time-domain (TD) DOT systems have been created with the ability to improve the quality of brain activation images. Although components from both TD-DOT and UHD-DOT systems combined with the use of microtechnology would theoretically allow for a DOT system with optimized image quality, such a system has not yet been designed. Thus, a TD-UHD Micro-DOT was simulated for imaging metrics using NeuroDOT in order to determine whether or not the system's predicted metrics improved upon current systems.

In this study, predicted mean full width at half maximum (FWHM) and localization error values of the hypothetical system were compared to existing values of high-density (HD) DOT and time-domain (TD) DOT systems to place the hypothetical system within the context of existing technology. It was found that the hypothetical system was predicted to possibly improve in areas of image resolution upon both HD-DOT and TD-DOT systems but was not predicted to improve upon the HD-DOT system in terms of localization error. These findings imply that the TD-UHD Micro-DOT system design must be improved in order to reduce localization error before it is built.

INTRODUCTION

Diffuse optical tomography (DOT) is a biomedical imaging technique that uses diffuse photons to determine the chemical composition of a sample. When used to image the brain, oxygen concentration values can be used to determine the magnitude of brain activity in cortical regions. The measuring of brain activity in naturalistic environments allows for a deeper understanding of cortical processes, which in turn allows for the development of treatments for patients affected by neurological conditions. DOT's unique ability to maintain naturalistic scenarios sets them apart from magnetic resonance imaging (MRI) systems, which cause stress to patients, creating inaccurate scans of baseline brain activity. However, DOT systems today have not yet been optimized to image with high quality and data accuracy while also maintaining patient comfort. Thus, in this study, a DOT system was designed to maximize image resolution while minimizing the bulkiness of the system. The conceptual design was simulated in a DOT simulation model to determine its advantages in terms of image quality. This study addresses whether or not the hypothetical system improves on current widespread systems, such as high-density (HD) DOT and time-domain (TD) DOT systems.

Non-Invasive Medical Imaging Systems

Over the span of 130 years, noninvasive medical imaging techniques have evolved from basic X-ray systems that create two-dimensional high-contrast images of bone structure (Panchbhai) to now being sophisticated mechanisms with a much larger scope of abilities (Hussain et al.). Today, modern systems such as magnetic resonance imaging (MRI) and computed tomography (CT) are capable of creating high-resolution, three dimensional renderings of a broad range of biological tissues and their intrinsic activity (Hussain et al.). An application for medical imaging techniques (predominantly MRI) of current focus is that of rendering brain activation (Laureys et al.); the utilization of biomedical imaging for neurological studies progresses research on a range of neurological complications and conditions such as Alzheimer's disease, stroke, and autism spectrum disorder (ASD) (Wheelock et al.), which sets the stage for the development of new treatments or therapies for those affected. However, despite the reputable benefits of MRI and CT, they tend to be cost prohibitive (Fred), uncomfortable for patients (Ghadimi & Sapra), as well as large and difficult to transport and maneuver (Hoshi & Yamada). In addition, the powerful magnets in MRI machines limit its application to patients without internal or external metallic implants (Ghadimi & Sapra). Thus, more accessible and user-friendly systems need to be developed in order to improve the identification of or treatments for neurological disorders.

Advantages of Diffuse Optical Tomography

A promising, cost-efficient, and mobile lightweight alternative (Bouchard et al.) to MRI and CT when rendering three-dimensional images of soft tissues is diffuse optical tomography (DOT) (Hoshi & Yamada). DOT systems utilize the principle of near-infrared spectroscopy (NIRs) (Hielscher et al.) to map levels of blood oxygen content and hemoglobin concentration; NIR are utilized due to their ability to penetrate biological tissues at desired depths and scatter upon making contact with certain substances (Hernandez-Martin & Gonzales-Mora). Because every biological tissue has its distinct scattering properties, DOT systems are able to use a configuration of LED sources and photodiode detectors to measure the light backscattered from a sample and analyze it for properties of biological tissues using analytical computation (Hernandez-Martin & Gonzales-Mora).

In the field of neuroimaging, DOT has shown promising and quality results in the field of imaging brain activation (Kim et al.). Although MRI also shares this ability, MRI systems are (1. largely expensive (Hoshi & Yamada), (2. not quick or easy to access (Hussain et al.), and also (3. fail to properly replicate (Zhou & Becker) or assess brain responses to stimuli in any naturalistic setting (Markow et al., "Identifying Naturalistic Movies"), due to discomfort (Ghadimi & Sapra) caused by the compressed patient/user structure (Tripathy et al., "Mapping Brain Function"). DOT, however, serves as a supplement for these issues (Markow et al., "Identifying Naturalistic Movies"). The lightweight and user-friendly structure of DOT systems causes minimal discomfort for patients when being used (Checkin et al.); DOT's ability to quickly generate images allows the viewing of tissue in real time (Schroeder et al.), making it an optimal technique for assessing brain activation in real-time simulated naturalistic scenarios (Schroeder et al.).

Importance of Scanning Brain Activation & Simulating a Naturalistic Environment

A naturalistic scenario is defined as a situation that is as similar to a normal day-to-day setting as possible (Zhou & Becker). These scenarios are created by producing familiar stimuli, such as conversation (Schroeder et al.) or movies (Markow et al., "Ultra High Density"), and introducing them to the patient (Markow et al., "Identifying Naturalistic Movies"). The importance of simulating a naturalistic environment lies within a base incentive for brain activity analysis: observing and studying brain function in patients affected by neurological diseases (Checkin et al.) or other complications (Kim et al.). In the past, MRI has previously been used to assess brain metabolism and productivity in patients subject to different neurological complications (Laureys et al.); unfortunately, it is a possibility that in assessments such as these, the neurological functions of certain patients may have adjusted to stimuli enforced by discomfort (Markow et al., "Identifying Naturalistic Movies") caused by the imaging system. This means that the activity imaged would be different from the base function exhibited in any natural situation (Zhou & Becker). Therefore, in order to properly study the naturalistic brain processes of certain patients, lightweight and user-friendly systems should be utilized in order to prevent skewed results caused by non-naturalistic scenarios. If researchers are able to collect accurate data on the impact of neurological conditions on brain activation, they can more effectively create the proper treatments for said conditions (Checkin et al.). Thus, using the lightweight and user-friendly DOT system would be optimal for imaging naturalistic brain activity (Fogarty et al.).

The Process of Brain Activation

Brain metabolic function is dependent on the cerebral blood flow (CBF), which carries oxygen to the brain (Hernandez-Martin & Gonzales-Mora). Cerebral blood vessels (blood vessels within the brain) interact closely with neurons, which are cells in the brain that receive and process information (Hernandez-Martin & Gonzales-Mora). Due to this close interaction, increased neuronal activity results in a greater amount of CBF (Hernandez-Martin & Gonzales-Mora). Because the CBF carries oxygen, an increase in neuronal activity is also synchronous with an increase of oxygen concentration in the brain. Thus, changes in activation within distinct areas of the brain are detected through the levels of oxygen concentration in that area (Hernandez-Martin & Gonzales-Mora).

DOT Functionality in Assessing Brain Activity

Because biological tissue is textured and non-uniform, photons are scattered or absorbed upon making contact with organic samples (Hernandez-Martin & Gonzales-Mora). The NIR utilized by DOT exist within the range of 690-850 nm wavelengths (Hernandez-Martin & Gonzales-Mora), which allow them to be absorbed by hemoglobin (HbO and HbR) in cerebral tissue (Fan et al.). The interaction of these rays with a sample depends on the scattering (the extent of how much light scatters through a medium) and absorption coefficients of the medium (the extent of absorption) (Hoshi & Yamada). The optical imaging of biological tissue relies heavily on the absorption of light by hemoglobin in the blood system due to its oxygen content (Kim et al.); utilizing wavelengths of 830 (Fogarty et al.) to 850 nm, changes of HbO concentration is calculated using the modified Beer-Lambert law (Hoshi & Yamada) on wavelengths of backscattered rays (Hernandez-Martin & Gonzales-Mora).

The NIR is sourced from source-detector (SD) (Custo et al.) pairs composed of (1. an LED (Tripathy et al., "Decoding Visual Information") or optic fiber light source and (2. a photodiode detector (Custo et al.). The detectors collect the distribution of backscattered photons that are adjusted to a curve trajectory (Uysal et al.) that approximates the depth at which the optical properties of the rays are altered by interacting with the sample (Hernandez-Martin & Gonzales-Mora). At an SD distancing of around 3-4 cm (Hernandez-Martin & Gonzales-Mora), backscattered photons contain information about both intracerebral and extracerebral (Hoshi & Yamada) layers of the brain. Data collected from attenuated NIR by detectors can then be mapped to a three-dimensional atlas (Checkin et al.) of the brain (Hoshi & Yamada) in which areas with greater levels of oxygen are those that are exhibiting greater levels of activity.

Limitations of DOT

Although DOT provides some advantage over other noninvasive imaging systems in the field of naturalistic brain scanning, it is limited by a lesser ability to create high-resolution (Custo et al.) images over greater depths (Hoshi & Yamada). Due to the great amount of scattering NIR exhibits upon making contact with tissue, DOT struggles with depth discrimination (Renehan et al.) and spatial resolution. This creates issues such as inaccurate data, high levels of noise, and an inability to image sub-cortical cultures (Hoshi & Yamada). In addition, some wearable DOT systems apply pressure on the sample, which skews data and returns inaccurate results (Checkin et al.). Therefore, more advanced DOT systems must be developed in order to supplement these disparities.

Iterations of DOT Systems

In response to the limitations of DOT, further research has been conducted to produce DOT systems with improved performance. Some examples include time-domain DOT systems (TD-DOT), Micro-DOT (Renehan et al.), and high density DOT systems (HD-DOT). Recent studies have shown that TD-DOT systems produce higher quality images of brain activation (Checkin et al.) than other DOT systems with standard density SD arrays due to their ability to collect data from a wider range of photonic attributes (Hoshi & Yamada), therefore making them optimal for imaging brain activation (Checkin et al.). TD-DOT systems can be configured with HD (high density) arrays (White & Culver) and an increased number of SD pairs to 126 (Markow et al., "Ultra High Density") to greatly improve image resolution (White & Culver).

Recent studies have also proven HD-DOT (Tripathy et al., "Decoding Visual Information") and UHD-DOT's (ultra high density) (Markow et al., "Ultra High Density") superior ability of rendering extremely high quality images. High density arrays allow for images of higher quality (White & Culver) and resolution by taking overlapping measurements (Tripathy et al., "Decoding Visual Information") at different distances; however, an increasing number of SD detectors (such as those which comprise a UHD system) in turn creates a larger, heavier system that can place non-naturalistic stress on the patient during a brain scan (Fogarty et al.). Recent research has shown that this problem can be solved by using microtechnology in order to configure a Micro-DOT system with components of the same principle (Renehan et al.); using sources and detectors of considerably lesser dimensions, Micro-DOT systems have the advantages of being (1. lighter and less stress inducing, (2. more portable, and (3. able to take higher quality and more accurate images due to the decreased spacing between SD pairs (Renehan et al.).

Designing and Simulating a TD-UHD Micro-DOT System

Hypothetically, a wearable whole TD-UHD Micro-DOT system would be optimal for rendering brain activation hence the advantages of each component. Although studies have been conducted on small-scale Micro TD-HD-DOT systems individually (Renehan et al.), there have not yet been any studies done on Micro TD-UHD DOT systems; nor have any been designed. Therefore, in this study, a Micro TD-UHD-DOT system was designed and simulated for brain scanning performance. Thus, the topic of inquiry for this study was: in accordance with the limitations of current DOT systems, would a TD-UHD Micro-DOT system have the potential to improve upon current technology for scanning brain activity in comparison to HD-DOT and TD-DOT systems based on predicted data accuracy and image resolution?

METHODS

Hypothetical TD-UHD Micro-DOT System

Because existing HD-DOT and UHD-DOT systems are bulky, heavy, and place stress on patients (Fogarty et al.), studies have been conducted to reduce system weight by using microtechnology to fit smaller, lighter SD pairs (Renehan et al.). This also increases space for more SD pairs to be implemented to construct high density imaging arrays (Renehan et al.). Previous studies have shown that by using ultra-high density SD arrays, UHD-DOT systems have the ability to image brain activity at a much higher resolution (Markow et al., "Ultra High Density") and much greater depth than traditional DOT systems (White & Culver). TD-DOT has also demonstrated a high ability to render clearer images of brain activity with lower levels of noise (Checkin et al.) through its ability to record a wide range of photonic attributes

(Hoshi & Yamada). Thus, it was hypothesized that because Micro-DOT technology allows for the use of layered UHD arrays at a smaller scale (Renehan et al.), a greater number of time-resolved TD-DOT SD pairs can be implemented around a model, which would render images of brain activation with optimally increased image quality, resolution and minimal error in comparison to existing TD-DOT and HD-DOT models.

Ethics & Institutional Review Board Exemption

This study did not include any human subjects or participants, however, I have received proper ethical training administered by my AP Research instructor. My study was exempt, reviewed, and accepted by the school's Institutional Review Board because it did not include any human subjects.

Simulation Modeling

The aim of this study was to assess the potential image quality of a hypothetical TD-UHD Micro-DOT system. In order to properly predict and assess the potential performance of the hypothetical instrument, simulation modeling was used to simulate the predicted optimal performance of the conceptual design in order to determine whether or not it had the potential to improve on current technology. Simulation modeling was the method of choice for this study because it provided insight into the expected performance of a hypothetical system (Menner, Markow et al., "Ultra High Density") and for the experimentation within a complex system (Menner) through the use of computer programs and digital modeling. The benefits of these characteristics lie within the manner of which complex technical instrument designs (Dahabreh et al., Maria) can be assessed for performance metrics before they are even constructed (Menner), which saves resources (Maria), time, and can prevent the construction of ill-performing instruments that do not improve on current systems (Dahabreh et al.). Simulation also reduces the chances of failure present in an existing system before it is built or altered, and allows for the studying of a design's optimal performance without the possibility of physical errors or operator mishaps (Maria).

Simulation modeling is the process of constructing a digital, conceptual abstraction of a system and facilitating experimentation within it (Menner) by using a computer program to assess the performance of a computerized design (Kleijnen). The conceptual model of the system mimics real-life conditions based on valid findings and pre-existing data (Dahabreh et al., Eggebrecht & Culver) in order to recreate the situation in a manner closest to reality using the system's related predictive mathematics (Menner). To simulate an experimental design, the conditions of said design must be implemented within the system computerized model (Maria). Computerized systems must also be validated and verified (Menner) to assess their closeness to reality (Kleijnen); this can be done by configuring the system model with known conditions and comparing the simulation results with the real-life outcome for a series of trials (Maria). This process ensures the correctness and consistency of the model (Maria, Menner) which helps justify simulation data under hypothetical conditions (Kleijnen).

After a system model is validated, an appropriate experimental design can be created, with which the conditions of said design are implemented within the computerized system model as input data (Maria). Multiple simulation runs of the model and its experimental conditions are then performed; 10 simulation trials were performed in this study in order to ensure confidence in the results as advised by past researchers (Jayawardana et al.). When using predictive software, simulation results (Maria) are often analyzed using statistical techniques such as mean and standard deviation (New York Institute of Technology). Generalizations made by these statistical models allow for predictions to be made about the experimental design's real world performance within an existing system (New York Institute of Technology, Kleijnen). Based on these predictions, further courses of action can then be given to future researchers in studying the experimental model or constructing a real-world configuration (Maria).

Previous DOT Simulation Studies

Past studies have been conducted using simulation modeling to predict the performance of hypothetical DOT systems in order to support the construction of the real-world instrument (Markow et al., "Ultra High Density", Fan et al., White & Culver). The assessment of predictive data and the modeling of the instrument provided the researchers in these studies with the information needed to justify constructing a real world model

Simulation is a crucial method for justifying hypotheses relating to experimental or conceptual designs (Menner); in addition to this advantage, simulation modeling has been proven to be proficient in supporting hypotheses regarding DOT designs, thus was used in this experiment to provide insight into the optimal performance of a hypothetical instrument.

NeuroDOT: DOT Toolbox

The simulation system of choice for this study was that of NeuroDOT (NeuroImaging Tools & Resources Collaboratory). NeuroDOT is a self-contained, multifaceted Python DOT simulation toolbox which contains functions for data processing, light modeling, image reconstruction, and the visualization of simulated brain activity (Speh et al., "NeuroDOT"). The toolbox also contains published DOT datasets from existing systems to reflect relevant experimental paradigms in neuroimaging and data quality metrics (Eggebrecht & Culver). Created by DOT researchers, NeuroDOT simulations are meant to replicate real-world DOT mechanics as closely as possible; the toolbox also allows for the visualization and 3D reconstruction of simulation data and data quality renderings (Eggebrecht & Culver). In this study, NeuroDOT was used to simulate data reconstruction and assess the image quality of a TD-UHD Micro-DOT system. Previous studies have already been conducted that validate and verify the consistency and correctness of NeuroDOT output data (Tripathy et al., "Mapping Brain Function", Yang et al.), meaning that NeuroDOT was already sufficient for this study and did not need to be re-assessed for validation. The NeuroDOT toolbox was chosen for this study because it provides all of the functions necessary for simulating the optimal performance of a TD-UHD Micro-DOT system (Tripathy et al., "Mapping Brain Function", Yang et al.).

Designing the Simulation Model

The conditions of the simulation were modeled as the defining components of a TD-UHD Micro-DOT system, such as the UHD optode array, the optode spacing, and the time-resolved photon counting system. UHD arrays differ from HD arrays by their difference in optode spacing; UHD arrays often have optode spacings of 6.5 mm or less (Markow et al., "Ultra High Density") while HD systems consist of spacings greater than 6.5 mm to less than 13 mm (Tripathy et al., "Decoding Visual Information"). UHD arrays have the ability to consist of a greater number of optodes due to their decreased spacing; demonstrated by a previous study (Markow et al., "Ultra High Density"), a UHD-DOT system with 126 optodes was observed to perform with optimal image quality, where on the other hand, an HD-DOT system using only 96 optodes produced images of a lower quality than that of the UHD-DOT system (Tripathy et al., "Decoding Visual Information"). These conditions serve as the input data for the simulation: 126 830 nm light sources, 126 time-resolved photodetectors, and 6.5 mm SD spacing.

The microtechnology aspect of the computerized design was conceptualized by the close SD spacing (Renehan et al.), and the TD-DOT aspect was simulated through the use of measurements over different increments of time; these time-separated measurements are meant to replicate TD-DOT measurements which use pulsing light sources so that detectors can calculate the time-of-flight of reflected photons (Markow et al., "Ultra High Density", Renehan et al.). This effect allows for passed time to be a measure of depth, which is what is being replicated in the simulation through the tracking of synthetic optics at specific time intervals. One hundred twenty-six SD pairs were chosen for this study due to previous UHD-DOT systems using the same UHD-array framework demonstrating the ability to create high definition images (Markow et al., "Ultra High Density"). The simulated design also had an SD spacing of 6.5 mm; this choice was influenced by previous standard UHD-DOT systems with said SD spacing optimized for high quality images using microtechnology (Markow et al., "Ultra High Density").

The NeuroDOT simulation (NeuroDOT_Py v1.2.0) (Speh et al., "NeuroDOT_Py") was run on a 13-inch 8-Core GPU MacBook Air using VSCode as the codespace. The simulation conditions were written in Python 3.8.8; many imported libraries were used, such as Matplotlib to create visualizations, SciPy and NumPy for technical computing, and Plotly to create graphs and charts (Speh et al., "NeuroDOT_Py"). Current versions of NeuroDOT are optimized for Python 3.8.8 (Speh et al., "NeuroDOT_Py"), which was why the version was used. GitHub Copilot (v.1.110) was used to debug, restructure, and repair faulty self-written code to ensure that it ran.

For this study, a function was written in Python to create a test activation object (Gaussian blob) and simulate the hypothetical system's optical interactions with the test object using code from the NeuroDOT library. Inside of this function, processes were written to simulate TD-DOT data by taking measurements over different increments of time to calculate the time-of-flight of synthetic photons, as well as simulate image resolution and localization error. Code was also written to simulate randomized levels of noise; a time-based seed was integrated which generated differing levels of noise for each trial. This amount of noise was then added to the end result of the simulation's performance values.

Image Reconstruction

This notebook performs reconstruction of fNIRS data.

You can download the notebook from the NeuroDOT_Py GitHub

```
# General imports
import sys
import math
import os
import shutil
import json

import sys
import math
import copy
import numpy as np
import matplotlib.pyplot as plt
import matplotlib.gridspec as gridspec
from scipy.io import savemat


import neuro_dot as ndot
```

Python

Figure 1: Imports required for running the simulation on VSCode. This code was already provided in the folder NeuroDOT_Py (Speh et al., "NeuroDOT_Py").

```
# use a time-based seed so repeated runs differ;
seed = int(time.time())
rng = np.random.default_rng(seed)
```

Figure 2: Code using NumPy's random number generator to create a randomized seed. The seed is time based, meaning that it will generate a different seed every time the simulation is run between a certain period of time. The randomized seed is meant to represent realistic levels of random Gaussian noise that interferes with system measurements. Random noise values will be added to the simulated performance of the system. This code was written with the assistance of GitHub Copilot.

It is important to simulate the effect of realistic levels of noise in order to conceptualize a stronger hypothesis of how the system might perform in a real-world setting. Because the seed changes for each trial, caused simulation runs to differ in performance values. The addition of noise and difference between trials is important because it allows for a more complete idea of the average performance of the system, not just how the system might perform in settings with fixed noise levels.

```
# timecourse
Nt = 40
amps = np.zeros(Nt)
amps[0:12] = 0.0
amps[12:28] = 1.0
amps[28:] = 0.0
```

Figure 3: Portion of the program which integrates the time-domain aspect into the simulation. The code displayed above simulates optical measurements across 40 discrete time intervals, which mirrors how TD-DOT systems use sources which emit timed light pulses so detectors can calculate the time-of-flight of photons. GitHub Copilot was used to assist in writing this portion of the code.

```
ysim = np.zeros((Nm, Nt), dtype=np.float64)
for t in range(Nt):
    xt = x_true * amps[t]
    with np.errstate(divide='ignore', over='ignore', invalid='ignore', under='ignore'):
        y = phi0 * np.exp(- (A @ xt))
    y = y + 1e-4 * rng.normal(size=y.shape)
    y[y <= 0] = 1e-9
    ysim[:, t] = y
```

Figure 4: The for loop displayed is used to create a matrix of time-domain measurements. The target object in this simulation is a simulated voxel activation. The variable ‘x_true’ represents the base activation vector, while the variable ‘true_center’ defines the ‘blob’ and spatial center of activation. The ‘ysim’ values are the simulated time-correlated measurements. GitHub Copilot was used to assist in writing this portion of the code.

```python
# --- compute FWHM from central slice radial profile ---
zs = np.unique(vox_coords[:, 2])
z_target = true_center[2]
zidx = int(np.argmin(np.abs(zs - z_target)))
zval = zs[zidx]
slice_mask = np.abs(vox_coords[:, 2] - zval) <= (mmppix[2] / 2.0 + 1e-6)
pts2d = vox_coords[slice_mask][:, :2]
vals2d = activation[slice_mask]
fwhm_mm = radial_fwhm_from_slice(vals2d, pts2d, mm_bins=60)
```

Figure 5: The code displayed simulates the full width at half maximum (FWHM) of the system in millimeters (mm). FWHM measures the width of the peak of the scanned activation signal/the distance between all points in the activation (created through modeling of optical interaction between the system and test object). The less wide the peak is, the greater the spatial resolution. The code simulates a radial profile around the peak of activation and returns the FWHM value. GitHub Copilot was used to assist in writing this portion of the code.

```python
try:
    flat = activation
    if np.all(~np.isfinite(flat)):
        raise RuntimeError('Activation all non-finite')
    peak_idx = int(np.nanargmax(flat))
    peak_coord = vox_coords[peak_idx]
    loc_error = float(np.linalg.norm(peak_coord - true_center))

    weights = flat.copy()
    weights[~np.isfinite(weights)] = 0.0
    W = np.sum(weights)
    if W <= 0:
        centroid = peak_coord
```

Figure 6: The code displayed simulates peak localization error by measuring the distance between the activation peak and the actual center of activation of the test object. The measurements were simulated through the modeling of optical interaction between the system and test object. ‘flat = activation’ is the reconstruction map, while ‘vox_coords’ is a matrix containing all voxel positions measured in millimeters (mm). GitHub Copilot was used to assist in writing this portion of the code.

The test object in this simulation was a Gaussian blob with an amplitude of 0.6 and a spatial extent of 6.0 mm. The time-domain aspect of the simulation was created by measuring the test object across 40 discrete time intervals within a single trial. FWHM values were then simulated by measuring the width of the activation signal, which depicts the spatial resolution capabilities of the hypothetical system. Localization error values were simulated by measuring the distance between the activation peak and the actual true center of the test object. The differing levels of noise generated by the randomized seed do not interact with the test object; instead, realistic levels of noise are added to the measurements of the system's simulated performance. Because the seed changes for each simulation run, FWHM and localization error values will differ for each trial. This variation in measurements allowed for a baseline understanding of how well the system could perform in a real-world situation where noise is variable. The FWHM and localization error values arise from a simulation of modeled optics, rather than properties of the test object. Because the synthetic test object is a perfect, smooth, and symmetrical Gaussian blob, the simulation produced values that would differ from real-world tests of a physical system. Biological tissue (for example, brain tissue) is textured, non-uniform, and asymmetric. The differences between the synthetic and real-world sample render simulation values as non-exact and therefore only a very loose prediction of the system's real-world performance.

A specific issue that can be caused by properties of the test object is that of inaccurate localization error value predictions. Because the Gaussian blob is sharper than real-world neural activations, the simulated system failed to precisely localize the center of activation. The test object also encompasses a smaller volume than real-world brain activation responses, which made it more difficult for the simulation to pinpoint its center of activation. The Lambda regularization in this study meant to smoothen noise from data reconstruction was set to a parameter of 0.1. The unitless parameter is meant to ensure smooth data without increasing FWHM values. The regularization model used to smoothen the data could have possibly over-regularized an already sharp Gaussian phantom. Real-world neural activations may regularize better due to their non-uniform and irregular shapes. This possible over-regularization of the test object could push the peak activation signal further from the object's true center of activation.

$$\bar{x} = \frac{\Sigma xi}{n} \qquad (1)$$

$$s = \sqrt{\frac{\Sigma(xi - \bar{x})^2}{n - 1}} \qquad (2)$$

For each of the 10 trials (Jayawardana et al.), simulated data was recorded for the hypothetical system's full width at half maximum (FWHM) and localization error (Markow et al., "Ultra High Density"); from these trials, the mean (1) and standard deviation (2) values of these properties were then calculated to provide generalized models of the instrument's predicted performance (New York Institute of Technology). The values for each trial differ due to the addition of noise added to the system's performance created by the randomized seed. Output data was stored in the coding workspace and then transferred to tables in Google Sheets; mean and standard deviation values were also stored in tables. These properties were chosen for comparison because they demonstrate the ability of a DOT system to reconstruct images of high quality and spatial resolution (White & Culver, Speh et al., "NeuroDOT"). FWHM is a resolution metric that measures the maximum separation between all points in the activation, with lower separations signaling higher spatial resolution (White & Culver). Localization error is the distance between the center of a sample point's image compared to the center of the actual target (White & Culver), with lower distances signaling higher data accuracy. Together, these two metrics define the effective resolution of the system (White & Culver). These values were then compared to the corresponding performance values of existing TD-DOT and HD-DOT values.

The existing TD-DOT and HD-DOT FWHM and localization error values serve as non-equivalent reference points. Because they were sourced from existing literature rather than being simulated in this study, they cannot serve as a direct reference to determine the advantages of the hypothetical system because they do not exist under the same conditions. The non-equivalence is mostly attributed to the test object to real world sample difference; because the sample used in this simulation was a perfectly symmetrical Gaussian blob, it cannot be directly used to predict real world performance. Instead, simulation data beside real world DOT values was meant to place the simulated values within the context of existing DOT system performances. Rather than to prove that the simulated system improves on current technology, the analysis places the simulated performance of the hypothetical system into the context of existing systems. Lower mean and standard deviation values for FWHM and localization error than the two existing systems determine if there is a possibility that the TD-UHD Micro-DOT system may improve upon current technology relating to image resolution and reconstruction. If an improvement is made, it can be said that a TD-UHD Micro-DOT system has the possibility to yield optimal image resolution for scanning brain activation in a naturalistic scenario.

RESULTS

Simulation Data

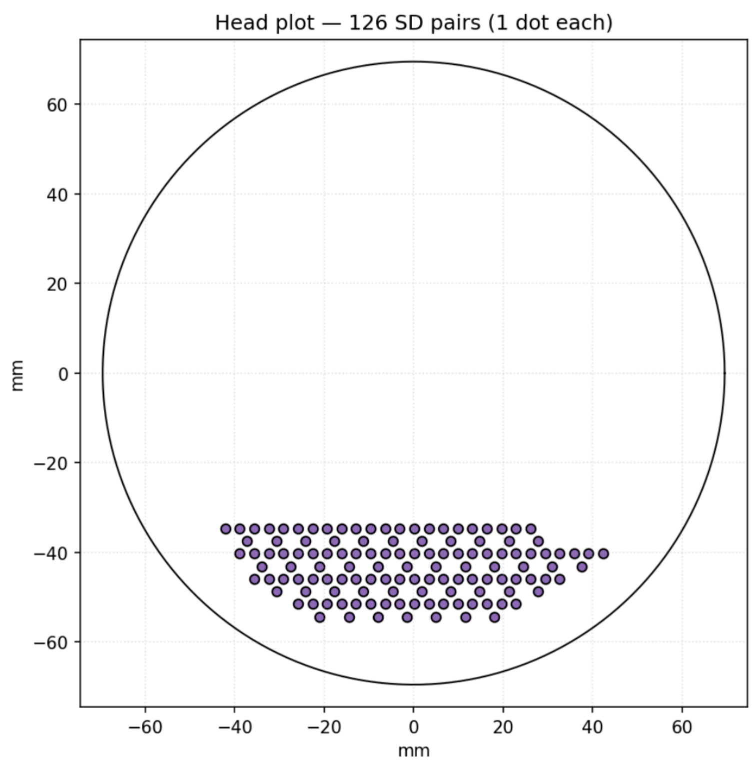

Figure 7: A conceptual representation of the TD-UHD Micro-DOT SD layout created using NeuroDOT including 126

SD pairs at a 6.5 mm spacing. The circle displayed in the diagram is a simplified representation of the brain. Each dot represents a singular SD pair, which includes the light source and the photodetector. GitHub Copilot was used to assist in the code that allowed for the creation of this file in NeuroDOT using Python.

Using the NeuroDOT toolbox, FWHM and localization error values were recorded for 10 simulation trials of the 126 SD pair TD-UHD Micro-DOT system. VSCode was used as the codespace, and each trial was saved to the disk of the Macbook Air.

Trial #	FWHM (mm)	Localization Error (mm)
1	10.2966	4.5592
2	9.8319	4.5861
3	10.3092	4.5592
4	10.3038	4.5592
5	10.3073	4.5592
6	10.3039	4.5592
7	10.2955	4.5592
8	10.2966	4.5592
9	10.3131	4.5592
10	10.3081	4.5592

Table 1: Simulated FWHM and localization error values for 10 trials.

In Table 1, the FWHM values for each simulation trial are shown to have been consistent with the mean. The values exist within the range of 9.8319 mm to 10.3131 mm, not exceeding a difference of 0.4812 between any 2 values. The FWHM is shown to maintain this consistency across each of the 10 trials. Localization error values appear to remain identical for 9 out of the 10 trials. Because these trials were run at different times, each trial had a different seed, meaning each trial received a different addition of noise. It could be possible that the previous drawbacks of the Gaussian blob allowed the Lambda regularization to smooth out any variability caused by noise in the localization error values, which is why the majority of the values were recorded as 4.5592 mm.

Mean & Standard Deviation Values for FWHM and Localization Error

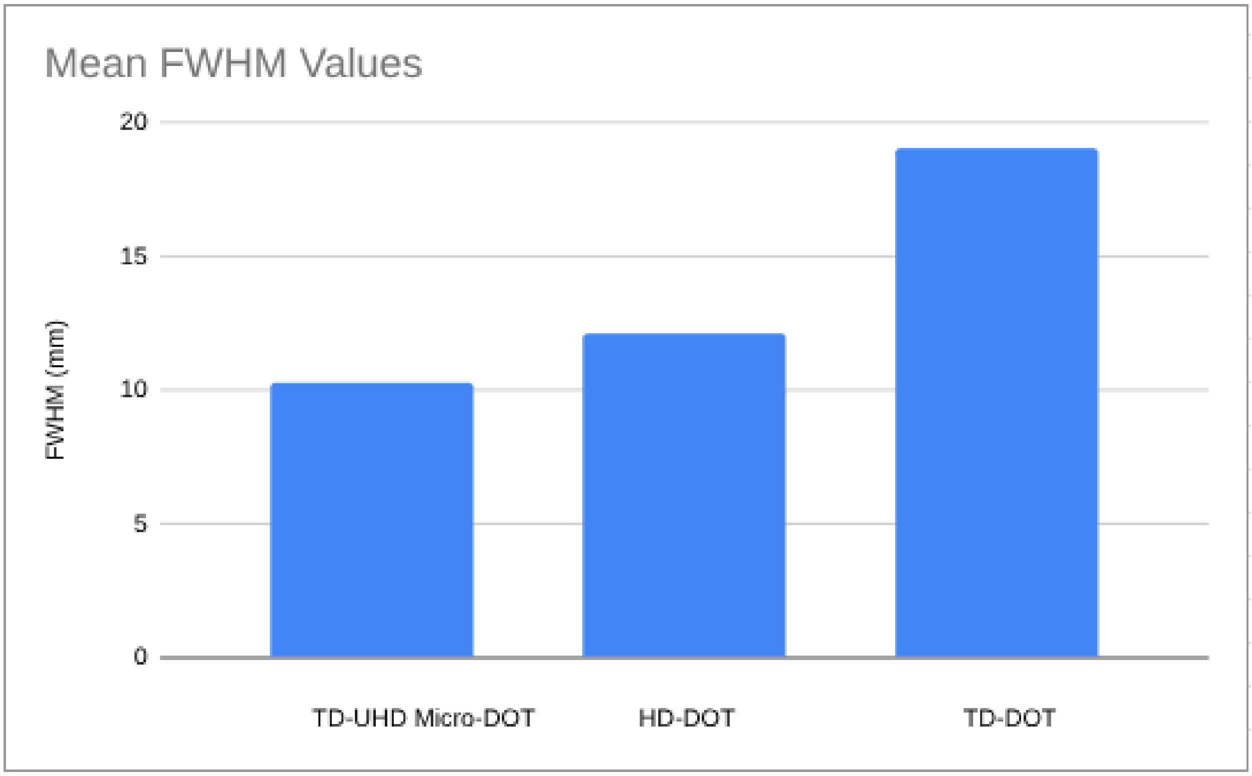

Figure 8: Mean FWHM (mm) values displayed in comparison; mean FWHM values (from left to right) are those of TD-UHD Micro-DOT, HD-DOT, and TD-DOT respectively. TD-DOT is displayed having the highest FWHM while TD-UHD Micro-DOT is displayed having the lowest.

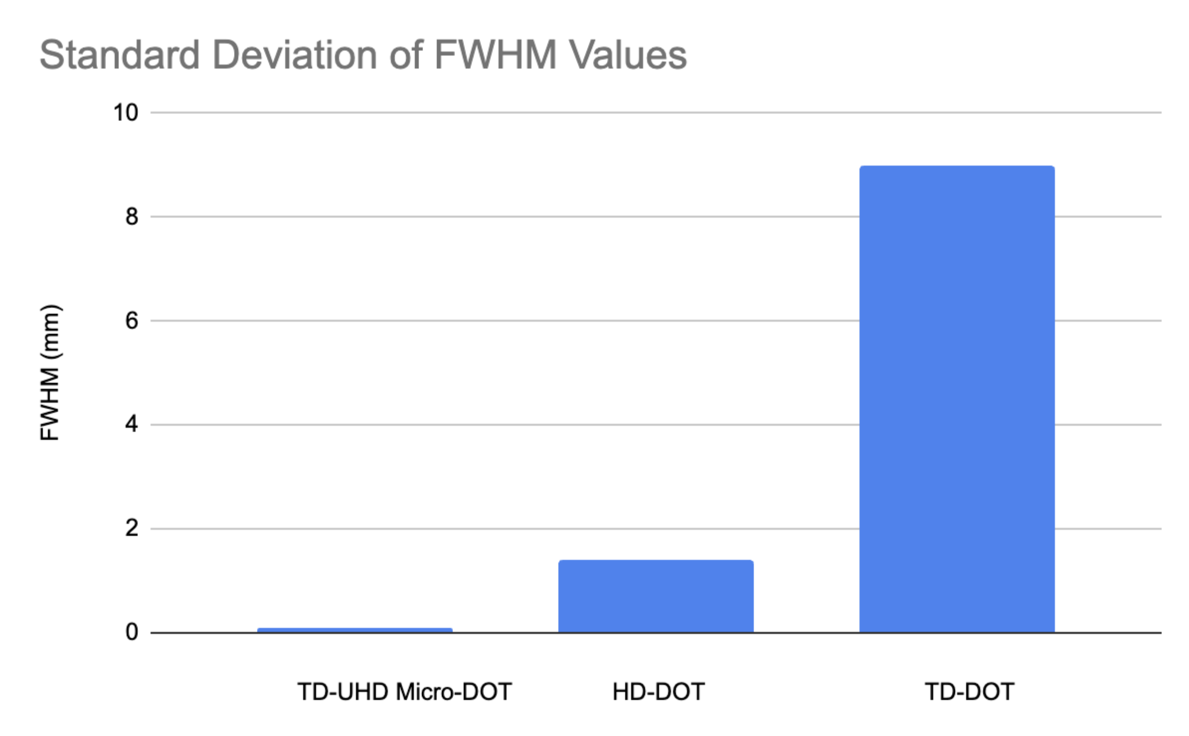

Figure 9: Standard deviations of recorded FWHM (mm) values displayed in comparison; standard deviations of FWHM values (from left to right) are those of TD-UHD Micro-DOT, HD-DOT, and TD-DOT respectively. TD-DOT is displayed having the highest standard deviation while TD-UHD Micro-DOT is displayed having the lowest.

System	Mean FWHM (mm)	FWHM Standard Deviation (mm)
TD-DOT	19.00	9.00
HD-DOT	12.10	1.40
TD-UHD Micro-DOT	10.26	0.0770

Table 2: Mean FWHM values for TD-DOT, HD-DOT, and TD-UHD Micro-DOT systems, along with their FWHM standard deviation values.

In Table 2, the mean value of FWHM for an existing TD-DOT system is displayed as 19.00±9 mm (Bouchard et al.), 12.10±1.40 mm for an existing HD-DOT system (White & Culver), and 10.26±0.0770 mm for the hypothetical TD-UHD Micro-DOT system. The mean value for FWHM of the TD-UHD Micro-DOT system was substantially lower than the mean values of the TD-DOT and HD-DOT systems, by 7.74 mm and 1.84 mm respectively. The standard deviation value for the TD-UHD Micro-DOT system's FWHM was also lower than the corresponding value for the other two systems, being 8.92 mm less than TD-DOT's standard deviation and 1.32 less than that of HD-DOT.

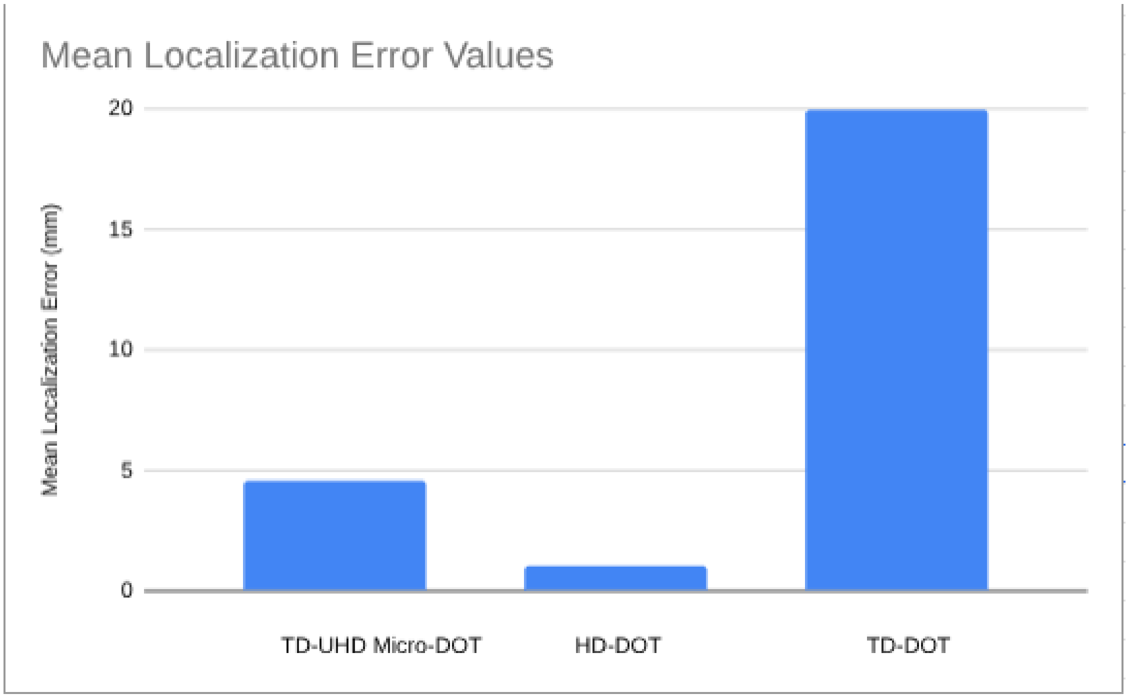

Figure 10: Mean localization error (mm) values displayed in comparison; mean localization error values (from left to right) are those of TD-UHD Micro-DOT, HD-DOT, and TD-DOT respectively. TD-DOT is displayed having the highest localization error, while HD-DOT is displayed having the lowest.

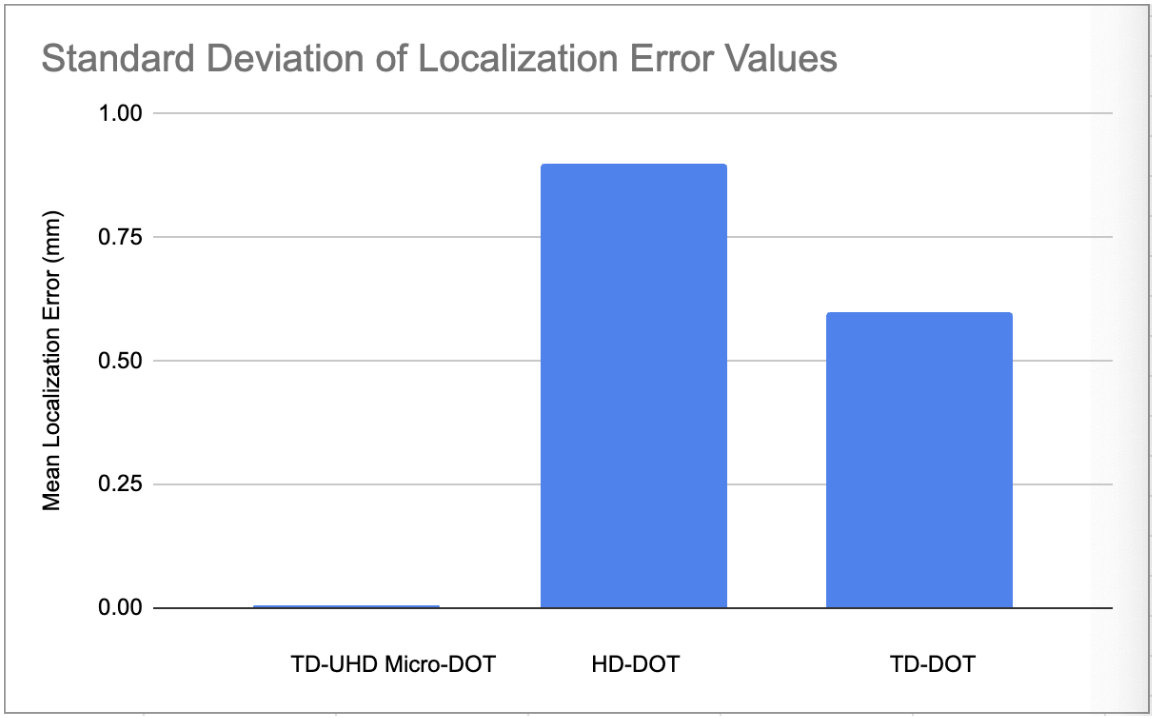

Figure 11: Standard deviations of localization error (mm) values displayed in comparison; standard deviations of localization error values (from left to right) are those of TD-UHD Micro-DOT, HD-DOT, and TD-DOT respectively. HD-DOT is displayed having the highest standard deviation, while the TD-UHD Micro-DOT is displayed having the lowest.

System	Mean Localization Error (mm)	Localization Error Standard Deviation (mm)
TD-DOT	20.00	0.6000
HD-DOT	1.000	0.9000
TD-UHD Micro-DOT	4.560	0.004402

Table 3: Mean localization error values for TD-DOT, HD-DOT, and TD-UHD Micro-DOT systems along with their standard deviation values.

In Table 3, the mean value of localization error for an existing TD-DOT system is displayed as 20.00±0.6000 mm (Checkin et al., Orive-Miguel et al.), 1.000±0.9000 mm for an existing HD-DOT system (White & Culver), and 4.560±0.004402 mm for the hypothetical TD-UHD Micro-DOT system. In this case, the mean localization error for the TD-UHD Micro-DOT system was less than the mean localization error value for TD-DOT by 15.44 mm, but greater than HD-DOT's corresponding value by 3.56 mm. The standard deviation value for the TD-UHD Micro-DOT system, however, was lower than that of the latter two systems, being less than that of TD-DOT's standard deviation by 0.59556 mm and less than that of HD-DOT by 0.8956 mm. However, the low variability of the TD-UHD Micro-DOT system's localization error can be attributed to the smooth shape of the Gaussian blob paired with the Lambda regularization over-regularizing the already uniform data. This issue may have caused the hypothetical system's standard deviation values to be fairly low. Regardless of the simulation, the real world system could possibly have much higher standard deviation values in relation to localization error.

Performance Comparison

Overall, the hypothetical TD-UHD Micro-DOT system was predicted to have the potential to outperform both the TD-DOT and HD-DOT systems in terms of FWHM. The TD-UHD Micro-DOT system had more consistent FWHM values than the latter two systems, hence its consistency around the mean value demonstrated by the standard deviation (9.0 mm >1.40 mm >0.0770 mm). In addition, the hypothetical system was predicted to have the potential to outperform the FWHM of the TD-DOT by a much larger proportion than that of HD-DOT (7.74 mm >1.84 mm). Having predicted a lower mean FWHM value than both systems (19.00 mm>12.10 mm >10.26 mm), it can be concluded that in terms of FWHM, the TD-UHD Micro-DOT system has the potential to outperform either system.

In regard to mean localization error, the hypothetical system outperformed the existing TD-DOT system (20.00 mm >4.56 mm), but not the existing HD-DOT system (4.56 mm >1.00 mm). Although the hypothetical system managed to have consistent values around the mean with a lower standard deviation than either of the other two systems (0.9000 mm >0.6000 mm >0.004402 mm), the mean localization error of the TD-UHD Micro-DOT system was higher than that of the HD-DOT system.

FWHM and Localization Error Interpretation

Lower FWHM values suggest that the DOT system renders sharper images with higher resolution (White & Culver), Thus, it can be said, at its optimal performance, the TD-UHD Micro-DOT system is predicted to possibly have low FWHM values which produce higher resolution images than existing HD-DOT and TD-DOT systems. Lower localization error suggests that the brain activation values are mapped accurately and do not deviate far from their actual location (White & Culver). According to this definition, the hypothetical system is predicted to have the ability to create more accurately mapped images than existing TD-DOT systems, but not existing HD-DOT systems.

DISCUSSION

Disproving The Initial Hypothesis

In this study, a conceptual model of a TD-UHD Micro-DOT system was created and simulated for FWHM and localization error values. The aim of this study was to compare simulated TD-UHD Micro-DOT parameters to existing TD-DOT and HD-DOT systems to determine whether or not the hypothetical system would improve on both existing systems in terms of image resolution and data accuracy.

The initial hypothesis for this study postulated that the simulated system would predict lower FWHM and localization error values than both the TD-DOT and HD-DOT systems, predicting a potential improvement upon current technology. However, after collecting and analyzing the data from all three systems, it was found that while the TD-UHD Micro-DOT system improved image quality in both cases, it failed to produce lower localization error values than the HD-DOT system. Thus, the hypothetical system is not predicted to have the ability to improve upon all aspects of current widespread DOT systems.

Implications of Research

Although the hypothetical system optimized image resolution, in this case, the TD-UHD Micro-DOT system would not be an optimal tool for imaging brain activation for all applications. The simulation predicted sufficient improvements upon the FWHM of current systems, highlighting its potential advantages in terms of image quality. However, localization error values for the system were less advantageous; the system could possibly improve upon current HD-DOT systems in terms of data accuracy if improvements were made to decrease localization error, such as the use of advanced regularization techniques in data reconstruction (Kavuri et al.).

Then again, high localization error values could possibly be attributed to the unrealistic shape of the test object. As previously stated, the Gaussian blob creates many disadvantages in the simulation process that can increase localization error values. If the simulation was done with a non-uniform, asymmetrical test object, there is a possibility that the regularization would be more successful and the simulated system would have an easier time locating the true center of the object. For a real-world application involving brain activation, there is also the possibility that localization error values would be completely different to those simulated in this study, possibly even lower than the predicted values, due to the non-uniform and asymmetrical shape of cortical blood vessels that are also more voluminous than the synthetic test object.

However, if these anomalous localization error values were not solely caused by the shape of the test object, it is also likely that they were caused by the minimal spacing between each optode paired with the large number of optodes comprising the system. Closer optode placement requires smaller voxel regularization than what was used in this study (Markow et al., "Ultra High Density"); standard regularization techniques do not have the ability to effectively resolve data collected by UHD-DOT arrays, which can lead to incorrect calculations and higher levels of localization error. If the localization error issues were caused by this reason, then it is also possible for these high error values to be reciprocated even in a real-world scenario with a non-uniform and voluminous sample.

There are also many issues that can cause higher levels of localization error that come with the use of UHD-DOT arrays. Because the optodes are placed with only 6.5 mm of separation, raw data can be corrupted or interfered with due to electronic cross talk in real-world applications (Markow et al., "Ultra

High Density"). The close optode spacing also causes decreases in the amount of light detected; the closeness of detectors prevents them from recording signals accurately, which can also increase localization error. These properties of UHD-DOT systems imply even greater issues with localization error separate to those demonstrated by the simulation performed in this study. Future researchers should take into note the drawbacks of UHD-DOT systems when considering the construction of a TD-UHD-Micro DOT system. Researchers should also consider implementing more advanced regularization strategies with the capacity to process UHD-DOT data, such as the combination of the Depth Compensation Algorithm (DCA) with the LASSO (L1) or L2 regularization techniques (Kavuri et al.).

Although it was not predicted to improve upon current HD-DOT systems in both areas, the hypothetical TD-UHD Micro-DOT system achieved a relatively low mean FWHM of 10.26±0.0770 mm, yielding the prediction that the system has the potential to be an optimal tool for enhanced image resolution over both HD-DOT and TD-DOT systems. The hypothetical system's predicted mean localization error value was also more than four times less than that of TD-DOT, which signals a possibility for significant improvement upon the existing system.

In a situation where an HD-DOT system does not utilize light-weight microtechnology and has a risk of producing an unnaturalistic scenario, the use of the TD-UHD Micro-DOT could possibly be advantageous. The lightweight system would have minimal risk of placing physical stress on the patient and was predicted to possibly have the ability to image brain activation at a greater resolution.

Filling The Gap

Simulating the instrument provided a prediction of TD-UHD Micro-DOT's image quality metrics, which enabled a prediction in its advantages if used to image brain activation. Because the simulated design predicted optimized FWHM over existing systems and relatively low localization error, it was hypothesized that a physical TD-UHD Micro-DOT system has the potential to serve as an effective alternative to current imaging systems in terms of image definition; not only would the system be a lightweight, user friendly device that allows for the imaging of brain activation within naturalistic environments, it could also potentially have optimized spatial resolution. An instrument as such could possibly provide a solution to the current lack of imaging systems with the ability to scan brain activity at a high resolution while also maintaining a naturalistic environment, which would benefit the development of effective treatments for patients with neurological conditions.

Limitations

Although this study provides somewhat of an understanding of the hypothetical TD-UHD Micro-DOT system's imaging metrics, the data from this study is purely hypothetical and serves as a prediction for the performance of the system. Thus, these findings cannot be used to directly describe the performance of the TD-UHD Micro-DOT system, but instead serve as a framework for the construction or re-simulation of future innovative DOT systems.

Issues mentioned previously in this study relating to the damaging effect of the synthetic test object, such as the over-regularization of data or the smooth, sharp shape of the object which creates a difficulty to pinpoint the actual center of activation, have potentially affected localization error values collected in this simulation. It is possible that the shape, small size, and smooth surface of the object increased localization error by making it more difficult for the regularization strategy to pinpoint the exact center of activation. Because the test object is smooth, symmetrical, and small, it differs greatly from real-world biological samples, such as cortical blood vessels, which also creates differences in the effectiveness of data regularization. This difference places a heavy limitation on this study; because the data collected in this study would possibly differ greatly from data collected during a real-world application, the data in this study can only be used as a very loose hypothesis rather than an accurate prediction. To further add to this discrepancy, many other factors that affect real-world DOT systems that were not included in the simulation can have an effect on data collected. For instance, electronic cross-talk and signal interference can have negative effects on data accuracy that were not accounted for in the simulation. It is also possible that low standard deviation values for both the FWHM and localization error of the hypothetical system can be attributed to the pairing of the smooth test object and the reduction in variability of already stable data through the Lambda regularization.

The possible difference between simulated data and real-world data created by these complications made it infeasible to compare simulated values to real-world data from existing studies. However, in this study, data from existing TD-DOT and HD-DOT systems was used to place the system into the context of current widespread DOT technology. This choice created a large limitation in the study; because the values synthesized from literature were from real-world DOT and not simulated data, they cannot be treated as equivalent reference points due to the differences between the simulation and real world scenario. Instead, the literature values were used to loosely place the simulated data within the context of real-world data, which in itself is counter-productive and only draws a weak connection between the simulated system and its existing counterparts.

When running the simulation, only 10 simulation trials were performed for this study, providing a small sample size that did not include outlying or abnormal values which could have affected the mean FWHM or localization error values collected. In addition, sections of code in the simulation were written by or debugged by GitHub Copilot and not by field professionals, meaning results could potentially be inaccurate due to faulty code.

Simulation results were also compared to HD-DOT metrics instead of UHD-DOT metrics, meaning that this study does not include any findings relating to the improvement of TD-UHD Micro-DOT systems upon experimental systems. This presents ambiguity around whether or not the hypothetical system improves upon an experimental DOT system rather than those with widespread use. In addition, because this study did not include participants or a physical system, there was no way to determine the extent to which the system allowed for the preservation of a naturalistic environment. Because previous studies

(Renehan et al.) using the same Micro-DOT array were shown to have preserved naturalistic brain function, it was thus assumed the system would have the ability to preserve a naturalistic environment.

Implications for Future Research

If looking to create a TD-UHD Micro-DOT system, future researchers should first work to improve certain aspects of the design that could reduce the localization error of images rendered. If such improvements are made, the system should be simulated and tested for imaging brain activity in real life applications; this would allow for accurate generalizations relating to the system's ability to image brain activation. The system's ability to maintain a naturalistic scenario should also be measured by comparing the brain activation imaged by the TD-UHD Micro-DOT system to systems which place stress on the patient, such as MRI. A performance comparison to MRI could potentially showcase the system's unique ability to maintain naturalistic scenarios all while rendering images with high quality.

Future researchers should also question the improvement of which the hypothetical system has over experimental systems such as UHD-DOT or TD-HD Micro-DOT systems. A comparison between the simulated resolution metrics of these experimental systems and the simulated data of the hypothetical system will allow for a more developed understanding of the system's improvement upon current technology. If looking to resimulate the system designed in this study, future researchers should use an irregular, textured shape with a greater size as the test object so that the complications created by using a Gaussian blob can be avoided. Because UHD-DOT systems require more advanced regularization techniques, the combination of the DCA with the L1 or L2 regularization techniques should be used to ensure accurate data reconstruction (Kavuri et al.). To compare the performance of the hypothetical systems to other existing systems, researchers should simulate the existing systems as well as the hypothetical system under the same conditions and compare these values with each other. This way, the simulated values of existing systems were tested under the same conditions, meaning they can serve as valid reference points. These points could allow for an analysis with the ability to accurately predict whether or not the hypothetical system improves upon current systems in terms of imaging resolution.

CONCLUSION

Current medical imaging technology is not yet optimized for imaging brain activation, particularly in scenarios where naturalistic stimuli and high resolution imaging must be maintained. In response, this review predicted how a hypothetical TD-UHD Micro-DOT system might perform in a synthetic environment in order to assess the potential image quality metrics of the system. The research conducted in this study aimed to provide a conceptual design for a hypothetical system which was hypothesized to have the potential to improve upon current medical imaging technology in terms of image resolution and data accuracy. A simulation of the system's imaging metrics was conducted in order to determine the strength of this hypothesis. This review highlights the potential advantages of a TD-UHD Micro-DOT system in terms of image quality, as well as potential drawbacks in terms of localization error. Drawbacks caused by the simulation design are also noted, particularly how the use of a Gaussian blob as a test object may have resulted in higher localization error values. This study implies the need for further research to be conducted relating to the system so that more accurate predictions can be made about its performance. In order to create more effective treatments for patients affected by neurological disorders, more research must be conducted on brain activation imaging technology to develop a greater understanding of neurological processes.

ACKNOWLEDGEMENTS

The author of this paper acknowledges that Figure 2 contains code edited and created by GitHub Copilot (v.1.110). Copilot was used to help structure the variables which defined the randomized seed with the ability to generate synthetic noise.

The author of this paper acknowledges that Figure 3 contains code edited and created by GitHub Copilot (v.1.110). Copilot was used to help create a system with the ability to simulate time-domain measurements. The section of code pictured was edited by Copilot so that measurements could be taken over a series of intervals.

The author of this paper acknowledges that Figure 4 contains code edited and created by GitHub Copilot (v.1.110). Copilot was used to help create a system with the ability to create a matrix of time-domain measurements, as well as a test object with the shape of a Gaussian blob.

The author of this paper acknowledges that Figure 5 contains code edited and created by GitHub Copilot (v.1.110). Copilot was used to structure and edit the section of the function in which FWHM was calculated through the simulation of a radial profile around the test object.

The author of this paper acknowledges that Figure 6 contains code edited and created by GitHub Copilot (v.1.110). Copilot was used to help structure and create the part of the function in which localization error values were simulated. Copilot helped program calculations that computed the distance between the predicted center of activation to the true center of activation (the center of the Gaussian blob).

The author of this paper acknowledges that Figure 7 contains an image created with code edited and created by GitHub Copilot (v.1.110). Copilot was used to help structure and create code that could create an image file to represent the design of the hypothetical system. Copilot did not create the design, rather, the author input the number of SD pairs into the code and Copilot helped structure the function which created the image file.

REFERENCES

Bouchard, Jonathan, et al. “A Low Cost Time-Correlated Single Photon Counting System for Multiview Time-Domain Diffuse Optical Tomography.” *IEEE Transactions on Instrumentation and Measurement*, vol. 6, no. 10, Oct. 2016, pp. 2505–15, https://doi.org/10.1109/TIM.2017.2666458. Accessed 6 Oct. 2025.

Checkin, Yaroslav, et al. “A Compact Time-Domain Diffuse Optical Tomography System for Cortical Neuroimaging.” *Imaging Neuroscience*, vol. 3, Jan. 2025, pp. 1–21, https://doi.org/10.1162/imag_a_00475. Accessed 6 Oct. 2025.

Custo, Anna, et al. “Anatomical Atlas-Guided Diffuse Optical Tomography of Brain Activation.” *NeuroImage*, vol. 48, no. 1, Jan. 2010, pp. 1–19, https://doi.org/10.1016/j.neuroimage.2009.07.03. Accessed 7 Oct. 2025.

Dahabreh, Issa J., et al. “Guidance for The Conduct and Reporting of Modeling and Simulation Studies in the Context of Health Technology Assessment.” *Methods Guide for Effectiveness and Comparative Effectiveness Reviews*, Oct. 2016, pp. 1–61, https://www.ncbi.nlm.nih.gov/books/NBK396066/#:~:text=Explicitly%20state%20the%20research%20question%20and%20the,guide%20the%20development%20of%20the%20mathematical%20model. Accessed 16 Jan. 2026.

Eggebrecht, Adam T. and Joseph P. Culver. “NeuroDOT: An Extensible MATLAB Toolbox for Streamlined Optical Functional Mapping.” *Proceedings of SPIE*, vol. 11074, July 2019, pp. 1–3, https://doi.org/10.1117/12.2527164. Accessed 16 Jan. 2026.

Fan, Weihao, et al. “Fundamental Effects of Array Density and Modulation Frequency on Image Quality of Diffuse Optical Tomography.” *Optica Biophotonics Congress: Biomedical Optics 2024*, June 2024, pp. 1045–57, https://doi.org/10.1364/TRANSLATIONAL.2024.JM4A.36. Accessed 7 Oct. 2025.

Fogarty, Morgan, et al. “Functional Brain Mapping Using Whole-Head Very High-Density Diffuse Optical Tomography.” *Imaging Neuroscience*, vol. 3, June 2025, pp. 1–23, https://doi.org/10.1162/IMAG.a.54. Accessed 7 Oct. 2025.

Fred, Herbert L. “Drawbacks and Limitations of Computed Tomography: Views From a Medical Educator.” *The Texas Heart Institute Journal*, vol. 31, no. 4, 2004, pp. 345–48, https://pmc.ncbi.nlm.nih.gov/articles/PMC548232/. Accessed 22 Oct. 2025.

Ghadimi, Maryam and Abi Sapra. “Magnetic Resonance Imaging Contradictions.” *StatsPearls*, May 2025, https://pubmed.ncbi.nlm.nih.gov/31869133/. Accessed 21 Oct. 2025.

Hernandez-Martin, Estefania and Jose L. Gonzales-Mora. “Diffuse Optical Tomography and in The Human Brain: A Briefly Review From the Neurophysiology to its Applications.” *Brain Sciences Advances*, vol. 6, no. 4, Feb.2021, pp. 289–305, https://doi.org/10.26599/BSA.2020.9050014. Accessed 7 Oct. 2025.

Hielscher, Andreas H, et al. “Near-Infrared Diffuse Optical Tomography.” *Disease Markers*, vol. 18, no. 5, Dec. 2003, pp. 313–37, https://doi.org/10.26599/BSA.2020.9050014. Accessed 7 Oct. 2025.

Hoshi, Yoko and Yukio Yamada. “Overview of Diffuse Optical Tomography and its Clinical Applications.” *Journal of Biomedical Optics*, vol. 21, no. 9, Sept. 2016, pp. 1–11, https://doi.org/10.1117/1.JBO.21.9.091312. Accessed 7 Oct. 2025.

Hussain, Shah, et al. “Modern Diagnostic Imaging Technique Applications and Risk Factors in The Medical Field: A Review.” *Biomed Research International*, June 2022, pp. 1–19 https://doi.org/10.1155/2022/5164970. Accessed 22 Oct. 2025.

Jayawardana, Kaushala S., et al. “A Practical Guide to Simulation for an Adaptive Trial Design With a Single Interim Analysis.” *Methodology*, vol. 26, no. 400, Oct. 2025, pp. 1–20, https://doi.org/10.1186/s13063-025-09100-5. Accessed 16 Jan. 2026.

Kavuri, Venkaiah C., et al. “Sparsity Enhanced Spatial Resolution and Depth Localization in Diffuse Optical Tomography.”*Biomedical Optic Express*, vol. 3, no. 5, Apr. 2012, pp. 943–57, https://doi.org/10.1364/BOE.3.000943. Accessed 16 Jan. 2026.

Kim, Hyun Keol, et al. “Ultrafast and Ultrahigh-Resolution Diffuse Optical Tomography for Brain Imaging with Sensitivity Equation Based Noniterative Sparse Optical Reconstruction (SENSOR).” *Journal of Quantitative Spectroscopy & Radiative Transfer*, vol. 26, Sept. 2021, pp. 1–32, https://doi.org/10.1016/j.jqsrt.2021.107939. Accessed 7 Oct. 2025.

Kleijnen, Jack P.C. “Verification and Validation of Simulation Models.” *European Journal of Operational Research*, 1995, pp. 145–62, https://doi.org/10.1016/0377-2217(94)00016-6. Accessed 16 Jan. 2026.

Laureys, Steven, et al. “Brain Function in Coma, Vegetative State, and Related Disorders.” *Lancet Neurology*, vol. 3, no. 9, Sept. 2004, pp. 537–46, https://doi.org/10.1016/S1474-4422(04)00852-X. Accessed 7 Oct. 2025.

Maria, Anu. “Introduction to Modeling and Simulation.” *Proceedings of the 29th Conference on Winter Simulation*, Dec. 1997, pp. 7–13, https://doi.org/10.1145/268437.268440. Accessed 16 Jan. 2026.

Markow, Zachary E., et al. “Identifying Naturalistic Movies from Human Brain Activity with High-Density Diffuse Optical Tomography.” *bioRxiv: The Preprint Server for Biology*, May 2024, pp. 1–12, https://doi.org/10.1101/2023.11.27.566650. Accessed 7 Oct. 2025.

———. “Ultra High Density Imaging Arrays in Diffuse Optical Tomography for Human Brain Mapping Improve Image Quality and Decoding Performance.” *Scientific Reports*, vol. 15, no. 1, Jan. 2025, pp. 1–16, https://doi.org/10.1038/s41598-025-85858-7. Accessed 8 Oct. 2025.

Menner, William A. “Introduction to Modeling and Simulation.” *Johns Hopkins APL Technical Digest*, vol. 16, no. 1, 1996, pp. 6–18, https://doi.org/10.1117/12.233059. Accessed 15 Jan. 2026.

NeuroImaging Tools & Resources Collaboratory. “NeuroDOT.” *NITRC,* 15 May 2026, https://www.nitrc.org/projects/neurodot/.

New York Institute of Technology. “Predictive Modeling & Statistical Analysis: Leveraging Data Science to Make Better Decisions.” *NYIT*, 11 Nov. 2023, https://online.nyit.edu/blog/predictive-modeling-statistical-analysis-leveraging-data-science-to-make-better-decisions#:~:text=Statistical%20Analysis%20Techniques,deviations%2C%20and%20other%20statistical%20measurements&text=Inferential%20Statistics:%20Draw%20insights%20by,observations%20made%20while%20gathering%20samples.

Orive-Miguel, David, et al. “Improving Localization of Deep Inclusions in Time-Resolved Diffuse Optical Tomography.” *Applied Sciences*, vol. 9, no. 24, Dec. 2019, pp. 1–27, https://doi.org/10.3390/app9245468. Accessed 3 Mar. 2026.

Panchbhai, Arati S. “Wilhelm Conrad Rontgen and The Discovery of X-Rays: Revisited After Centennial.” *Journal of Indian Academy of Oral Medicine and Radiology*, vol. 27, no. 1, Mar. 2015, pp. 90–95, https://doi.org/10.4103/0972-1363.167119. Accessed 22 Oct. 2025.

Renehan, Kevin, et al. “Wearable High-Density Time-Domain Diffuse Optical Tomography Array for Functional Neuroimaging.” *bioRxiv: The Preprint Server for Biology*, Apr. 2025, pp. 1–60, https://doi.org/10.1101/2025.04.22.649003. Accessed 8 Oct. 2025.

Schroeder, Mariel L., et al. "Mapping Cortical Activations Underlying Covert and Overt Language Production Using High-Density Diffuse Optical Tomography." *NeuroImage*, vol. 276, Aug. 2023, pp. 1–15, https://doi.org/10.1016/j.neuroimage.2023.120190. Accessed 8 Oct. 2025.

Speh, Emma, et al. "NeuroDOT: A MATLAB and Python Toolbox for Diffuse Optical Tomographic Brain Mapping." *Proceedings of SPIE*, vol. 13314, Mar. 2025, pp. 1–5, https://doi.org/10.1117/12.3040072. Accessed 16 Jan. 2026.

———. "NeuroDOT_Py v1.2.0." *GitHub*, 24 Oct. 2024, https://github.com/WUSTL-ORL/NeuroDOT_py/releases.

Tripathy, Kalyan, et al. "Decoding Visual Information From High-Density Diffuse Optical Tomography Neuroimaging Data." *NeuroImage*, vol. 226, Feb. 2021, pp. 1–16, https://doi.org/10.1016/j.neuroimage.2020.117516. Accessed 8 Oct. 2025.

———. "Mapping Brain Function in Adults and Young Children During Naturalistic Viewing With High-Density Diffuse Optical Tomography." *Human Brain Mapping*, vol. 45, no. 7, May 2024, pp. 1–24, https://doi.org/10.1002/hbm.26684. Accessed 8 Oct. 2025.

Uysal, Husamettin, et al. "Effect of Optode Geometry and Regularization Methods on Low-Cost Diffuse Optical Tomography Systems." *Optical and Quantum Electronics*, vol. 55, no. 1, Dec. 2022, pp. 1–24, https://doi.org/10.1007/s11082-022-04366-4. Accessed 8 Oct. 2025.

Wheelock, Muriah D., et al. "High-Density Diffuse Optical Tomography for Imaging Human Brain Function." *Review of Science Instruments*, vol. 90, no. 5, May 2019, pp. 1–24, https://doi.org/10.1063/1.5086809. Accessed 22 Oct. 2025.

White, Brain R. and Joseph P. Culver. "Quantitative Evaluation of HIgh-Density Diffuse Optical Tomography: In Vivo Resolution and Mapping Performance." *Journal of Biomedical Optics*, vol. 15, no. 2, Apr. 2010, pp. 1–14, https://doi.org/10.1117/1.3368999. Accessed 8 Oct. 2025.

Yang, Dalin, et al. "Mapping Brain Function Underlying Naturalistic Motor Observation and Imitation Using High-Density Diffuse Optical Tomography." *Imaging Neuroscience*, vol. 3, Sept. 2025, pp. 1–21, https://doi.org/10.1162/IMAG.a.153. Accessed 16 Jan. 2026.

Zhou, Feng and Benjamin Becker. "Understanding Human Brain Function in Real-World Environments." *PLoS Biology*, vol. 23, no. 6, June 2025, pp. 1–4, https://doi.org/10.1371/journal.pbio.3003210. Accessed 22 Oct. 2025.

ABOUT THE AUTHOR

Cemantha Hearing is a high school senior at Oswego High School in Oswego, Illinois. She is interested in the intersection of applied physics and medical technology and hopes to pursue a future career in applied physics research.